

# Kinetic Study of Homogeneous Alkene Hydrogenation by Model Discrimination

Lasse Greiner,<sup>a,\*</sup> Michel Brik Ternbach<sup>b</sup>

<sup>a</sup> Institut für Technische und Makromolekulare Chemie, RWTH Aachen, Worringerweg 1, 52072 Aachen, Germany

Fax: (+49)-241-802-2177, e-mail: l.greiner@itmc.rwth-aachen.de

<sup>b</sup> Institut für Biotechnologie, Forschungszentrum Jülich GmbH, 52425 Jülich, Germany

Received: December 2, 2003; Revised: June 25, 2004; Accepted: July 2, 2004

Supporting Information for this article is available on the WWW under <http://asc.wiley-vch.de/>.

**Abstract:** Model discrimination is one of the methods of choice to obtain a valid kinetic description of a catalytic reaction with minimal experimental effort. It allows fast judgement of catalyst behavior and its suitability for process development. Using dynamic experiments and modeling, the kinetics of a homogeneous hydrogenation with cationic rhodium-PyrPhos  $\{[\text{Rh}(\text{PyrPhos})(\text{COD})]\text{BF}_4\}$  were investigated. A set of three batch experiments allowed the discrimination

between 6 models. Qualitative and quantitative descriptions of the kinetic behavior could be derived. Most importantly, evidence for catalyst deactivation was gained.

**Keywords:** deactivation; dihydrogen; homogeneous catalysis; hydrogenation; model discrimination; simulation

## Introduction

Hydrogenation with transition metal complexes is among the best studied and developed fields of homogeneous catalysis.<sup>[1]</sup> In spite of this, only a small number of these processes has evolved so far for the enantioselective production of fine chemicals on larger scale.<sup>[1,2]</sup> Among other factors, a lack of quantitative kinetic descriptions under catalytic conditions is named as a reason.<sup>[3]</sup>

A thorough kinetic description of catalytic systems allows optimization of reaction conditions in order to improve the stability and activity of the catalyst as expressed by total turnover number and turnover frequencies, respectively.<sup>[3]</sup> Whereas a number of studies on the effect of hydrogen pressure and mass-transfer on the selectivity of homogeneous catalytic hydrogenations have been reported,<sup>[4]</sup> kinetic studies are rare.<sup>[3,5]</sup>

Description of the kinetics of homogeneous catalysis faces several difficulties. The use of initial rate measurements is often problematic as the true catalyst is first formed from a precatalyst species. Therefore, the concentration of active catalyst is a function of time and true initial rates may not be accessible. This activation may be a complex phenomenon, heavily depending on experimental conditions, e.g., mass transfer and substrate to catalyst ratio.<sup>[6]</sup> To be undisturbed by such activation phenomena, commonly a large excess of starting material has to be employed in order to reach the maximum reaction rate after activation. In contrast, relative-

ly low concentrations are necessary to obtain complex-binding constants from initial rates.

Furthermore, conversion data from small numbers of samples of dynamic experiments are often insufficient to support even a simplified model and alternative models may seem equally valid. It is advantageous to use on-line techniques with higher sampling rates to obtain a good basis for dynamic modeling.<sup>[7]</sup>

In this paper, we report the simulation of dynamic kinetic models to batch reactor data. The homogeneous hydrogenation of *N*-acetylaminocinnamic acid (**2**) by a PyrPhos-based rhodium complex<sup>[8]</sup>  $\{[\text{Rh}(\text{PyrPhos})(\text{COD})]\text{BF}_4$ ; **1-COD** $\}$  was used as a model system. The reaction was monitored in a constant pressure reaction autoclave by measuring hydrogen uptake rate on-line. Various models were fitted to experimental hydrogenation rates to obtain the best kinetic description *via* model discrimination.<sup>[9]</sup>

## Results and Discussion

The investigated catalyst is the rhodium(I) complex of the pyrrolidine-based diphosphine ligand PyrPhos and cyclooctadiene with tetrafluoroborate as counterion  $\{[\text{Rh}(\text{PyrPhos})(\text{COD})]\text{BF}_4$ , **1-COD** $\}$ .<sup>[8]</sup> The catalyst **1** is liberated from the precatalyst complex and catalyzes the hydrogen-consuming main hydrogenation reaction of **2** to the phenylalanine derivative **3** (Figure 1).

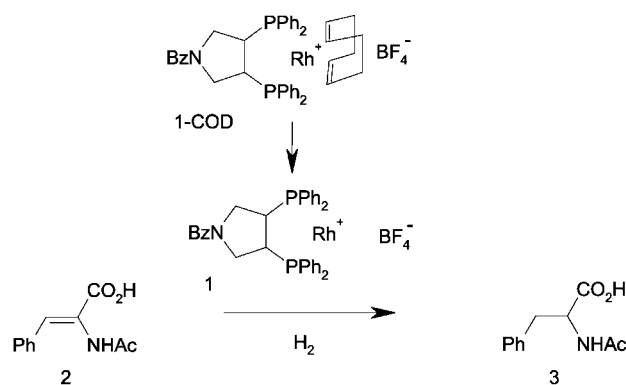


**Figure 1.** Simplified reaction scheme for the hydrogenation of 2-*N*-acetylaminocinnamic acid (**2**) to *N*-acetylphenylalanine (**3**) by catalyst **1**, which is liberated from its COD complex **1-COD**.

**Table 1.** Symbols and abbreviations.

Symbol	Usage	Unit
[A]	concentration of substance A	mmol L <sup>-1</sup>
<i>D</i>	denominator of Equation (2)	mmol L <sup>-1</sup>
<i>k</i> <sub>act</sub>	rate constant for catalyst activation	h <sup>-1</sup>
<i>k</i> <sub>deact</sub>	rate constant for catalyst deactivation	h <sup>-1</sup>
<i>K</i> <sub>2</sub>	complex binding constant for 2	mmol L <sup>-1</sup>
<i>K</i> <sub>i,A</sub>	inhibition constant for A	mol L <sup>-1</sup>
<i>v</i> <sub>max</sub>	limiting reaction frequency	mmol L <sup>-1</sup>

Six different dynamical models were fitted to the measured hydrogen uptake rates of the system per used volume (symbols and abbreviations in Table 1). The measured values were weighed by the estimated standard deviations which were  $7.0 \cdot 10^{-4}$ ,  $5.0 \cdot 10^{-4}$  and  $11 \cdot 10^{-4}$  for experiments 1, 2 and 3, respectively.

All models presume irreversible first order kinetics for the activation of the catalyst:

$$d[\mathbf{1-COD}]/dt = -k_{\text{act}}[\mathbf{1-COD}] \quad (1)$$

A fraction of the catalyst was assumed to be already in the active form **1** at the beginning of the experiment. This fraction was estimated as an extra parameter for each experiment.

All models are hyperbolic in the concentration of **2** and share the same nominator as the driving force of the reaction.

$$d[\mathbf{2}]/dt = -v_{\text{max}}[\mathbf{1}][\mathbf{2}]/D \quad (2)$$

Denominator *D* reflects adsorption equilibria of the catalyst with the reaction partners. The different denominators for each model are given in Table 2.

To account for the deactivation of active catalyst, a first order irreversible decay to an inactive form was assumed and combined with simple Michaelis–Menten kinetics (model 1) to give model 5. Analogously, combination of model 4 taking into account inhibition of both substrate and product gave model 6. The respective equations formed the system of ordinary differential equations for each model.

$$d[\mathbf{1}]/dt = +k_{\text{act}}[\mathbf{1-COD}] - k_{\text{deact}}[\mathbf{1}] \quad (3)$$

Initial concentrations of substrate **2** were estimated within 95–105% of the amount which was weighed in for each experiment, because of the strong sensitivity of the results of the simulation with respect to this concentration in the final phase of the experiments. Conversion of the substrate was found to be quantitative in each experiment as determined independently by capillary electrophoresis. This complete conversion at the end of the experiment is met by the simulations with the estimated adjusted initial concentrations.

The parameters of the respective system of ordinary differential equations of all models fitted to the three experiments simultaneously are shown in Table 3 together with the 95% accuracy limits.

Even though the mechanism of the hydrogenation is most likely to be more complex, the kinetics can be described rather well by the simplified rate equations,<sup>[5]</sup> under the boundary conditions of our experiments (constant hydrogen pressure/concentration and temperature). This also holds for the simple first-order deactivation of the catalyst where a much more complex deactivation route is likely as shown for the DIOP ligand.<sup>[10]</sup>

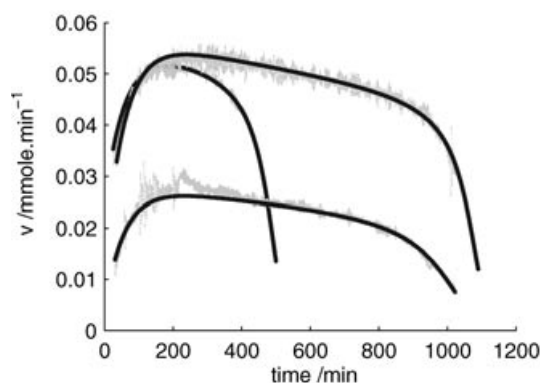
The difference between model predictions and measurements was weighed by the standard deviation and vi-

**Table 2.** Denominators *D* in Equation (2) and whether equation (3) for deactivation was included in the model.

Model	<i>D</i> in Equation (2)	Eq. (3)	Description
1	<i>K</i> <sub>2</sub> + [2]	–	Michaelis–Menten kinetics
2	<i>K</i> <sub>2</sub> + [2](1 + [2]/ <i>K</i> <sub>i,2</sub> )	–	substrate surplus inhibition
3	<i>K</i> <sub>2</sub> (1 + [3]/ <i>K</i> <sub>i,3</sub> ) + [2]	–	competitive product inhibition
4	<i>K</i> <sub>2</sub> (1 + [3]/ <i>K</i> <sub>i,3</sub> ) + [2](1 + [2]/ <i>K</i> <sub>i,2</sub> )	–	both inhibition types
5	<i>K</i> <sub>2</sub> + [2]	+	as model 1 but with deactivation
6	<i>K</i> <sub>2</sub> (1 + [3]/ <i>K</i> <sub>i,3</sub> ) + [2](1 + [2]/ <i>K</i> <sub>i,2</sub> )	+	as model 4 but with deactivation

**Table 3.** Parameter estimates with the estimated 95% accuracy bounds and reduced  $\chi^2$  values. (<sup>‡</sup> these values are at the upper boundary).

Model	1	2	3	4	5	6	Unit
$k_{\text{act}}$	$1.541 \pm 0.012$	$1.566 \pm 0.012$	$1.403 \pm 0.010$	$1.404 \pm 0.010$	$1.045 \pm 0.007$	$1.103 \pm 0.008$	$\text{h}^{-1}$
$k_{\text{deact}}$	–	–	–	–	$0.012 \pm 9 \cdot 10^{-5}$	$0.012 \pm 13 \cdot 10^{-5}$	$\text{h}^{-1}$
$K_2$	$25.3 \pm 0.11$	$27.4 \pm 0.18$	$5.96 \pm 0.17$	$7.61 \pm 0.21$	$17.6 \pm 0.09$	$20.5 \pm 0.23$	$\text{mmol L}^{-1}$
$v_{\text{max}}$	$10.8 \pm 0.006$	$11.0 \pm 0.013$	$10.7 \pm 0.005$	$10.9 \pm 0.012$	$11.6 \pm 0.009$	$12.0 \pm 0.019$	$\text{min}^{-1}$
$K_{i,2}$	–	$40^{\ddagger}$	–	$40^{\ddagger}$	–	$14.8 \pm 0.45$	$\text{mol L}^{-1}$
$K_{i,3}$	–	–	$0.177 \pm 0.007$	$0.221 \pm 0.008$	–	$11.8 \pm 2.6$	$\text{mol L}^{-1}$
$\chi^2$	7.0	6.8	4.3	4.2	3.4	3.0	

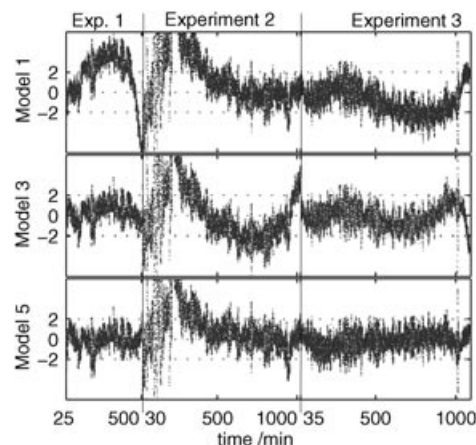
**Figure 2.** Experimental data (dots) and simulation according to model 5 (straight line).

sualized in a residual plot (Figure 3). Due to weighing, more than 95% of the residuals from well-fitting models should lie in the interval  $[-2;2]$ . Proper models should furthermore not show trends in their residual plots. Clearly, the deviation between model prediction and measured values is systematic for models which do not take into account deactivation [Equation (3)] (models 1–4) (Figure 3). Especially, simulated rates towards the end of the experiments deviate significantly from measured values.

The substrate inhibition constants  $K_{i,2}$  for models 2 and 4 are at the upper boundary of the allowed parameter space and do not have a significant influence on the course of the simulation. All inhibition constants for both substrate surplus and product inhibition are generally too large to be physically meaningful, especially when compared to substrate complex binding constants  $K_2$  which are at least 29 times smaller and were fitted within the same boundaries. Furthermore, parameters  $K_{i,3}$  and  $K_2$  are strongly correlated in models 3 and 4 (correlation coefficients  $> 0.98$ , data not shown).

The model which describes the course of the reaction without systematic deviations with the minimum number of parameters is model 5 (Figure 2): a Michaelis–Menten type model with deactivation of the catalyst and without inhibition.

The reduced  $\chi^2$  values confirm that the models with deactivation (i.e., model 5 and 6) perform best (Table 2).

**Figure 3.** Weighed residuals of models 1, 3, and 5 for all measured values of the three experiments

Model 6, with inhibitions, fits slightly better than model 5. Model 6, however, uses 2 parameters more than model 5, and the values of these inhibition constants are too high to be physically meaningful.

Better discrimination between the models 5 and 6 should be possible at higher substrate concentrations. Simulation of the models with initial substrate concentrations of more than  $2 \text{ mol L}^{-1}$  show significant difference in the predicted reaction rates (data not shown). However, the solubility limit of **2** is approximately  $1.2 \text{ mol L}^{-1}$  (methanol,  $20^\circ\text{C}$ ), so that experimental verification is not possible in this way. At and below the solubility limit models 5 and 6 predict practically identical rates.

## Conclusion

Model discrimination using simulation of dynamic models, together with on-line measurement of reaction rates, provides a powerful tool for the investigation of the kinetics of homogeneous catalytic reactions. By this means a system in which initial rates are not accessible was investigated.

Model discrimination reveals that the investigated catalyst is unstable under the reaction conditions. The

fit of models taking into account first-order deactivation shows best results in describing the course of the reaction. For continuous processes, the stability of the catalyst must be higher than that resulting from deactivation of  $k_{\text{des}} = 0.012 \text{ h}^{-1}$ . The corresponding half life time of  $t_{1/2} \approx 58 \text{ h}^{[11]}$  did not favor further efforts aiming for continuous catalysis.

As all experiments reach quantitative conversion within a reasonable time, a less detailed kinetic investigation would have missed deactivation of catalyst. Thus, combination of on-line monitoring and kinetic modeling points out catalyst robustness under truly catalytic conditions. This result emphasizes that development of new homogeneous catalysts should be accompanied by thorough kinetic investigations at an early stage.

## Experimental Section

Methanol, *N*-acetylaminocinnamic acid (**2**), and both enantiomers of *N*-acetylphenylalanine (**3**) were obtained in analytical grade from Sigma (Taufkirchen, Germany). Gases were of 99.9990% purity and obtained from Messer (Krefeld, Germany). PyrPhos-based rhodium cyclooctadiene (COD) {[Rh(PyrPhos)(COD)]BF<sub>4</sub> complex; **1-COD**} as tetrafluoroborate salt was a kind gift of Degussa AG, Hanau, Germany.<sup>[8]</sup> Conversion and enantiomeric excess were determined by capillary electrophoresis<sup>[12]</sup> {Beckman Pace/MDQ equipped with an uncoated fused silica capillary (Supelco CElectFS25, Sigma-Aldrich, Taufkirchen, Germany) (length to detection window 50 cm, total length 57 cm) in a 125 mmol L<sup>-1</sup> potassium phosphate buffer at pH 10.2 containing 25 mmol L<sup>-1</sup> dimethyl- $\beta$ -cyclodextrin, 16 °C, 30 kV, migration times: **2** 13.4 min, **3**: *S* 14.1 min, *R* 14.3 min}. Solvents were degassed prior to use by purging with helium and argon. Sensitive compounds were handled using standard Schlenk-type techniques.

Conversion of the substrate was found to be quantitative in each case as determined by capillary electrophoresis. The enantioselectivity of the reaction was confirmed to be pressure-independent (enantiomeric ratio 32, enantiomeric excess 94%).<sup>[8]</sup> The hydrogenation was investigated in a constant pressure autoclave (Mechanical Workshop of the Institute of Biotechnology, Forschungszentrum Jülich, Germany). The stainless steel autoclave (100 mL total volume) was equipped with a glass insert and magnetic stirring bar. The reaction vessel was charged with substrate **2** evacuated (<0.1 mbar) and purged with argon three times, before the precatalyst **1-COD** in 50 mL of methanol was transferred into the reactor under positive argon pressure. The reaction mixture was stirred to bring **2** into solution (2–3 min as determined by independent experiments). The reactor was then pressurized with hydrogen and tested for leakage. The reaction was started by stirring with an external magnetic stirrer. The autoclave was equipped with electronically controlled pressure and mass flow controllers (Bronkhorst, Rurloo, Netherlands). By this means a constant pressure was maintained (deviation less than 1% during reactions) and the hydrogen uptake of the system was monitored. Once the reaction mixture is saturated with hydrogen the uptake rate equals the reaction rate due to reaction stoichiometry. Data storage and control of the system were performed on a

personal computer with software written in LabView (National Instruments, Austin, USA).

## Modeling

Modeling was performed in Matlab/Simulink (The Mathworks) on a personal computer. The models were limited to describe the system at constant pressure (10 bar) in methanol at 25 °C. Models were fitted to experimental data of three experiments simultaneously. Experiments differed in the starting concentration of substrate (0.46 M, 0.46 M, and 1.00 M in experiments 1, 2 and 3, respectively) and catalyst (0.10 mM, 0.05 mM, and 0.10 mM in experiments 1, 2 and 3 respectively). The experiments were carefully chosen to be free from mass transfer limitations.

The measured data were used as obtained without smoothing. Measured data from the initial period of each experiment during which the flow control settled, typically about 30 minutes, were discarded before fitting the models to the data.

The model parameters were estimated by minimizing the sum of squares of the deviations between the measured and simulated hydrogen consumption rates, weighed by the standard deviations of the measured values. For each experiment, a constant absolute value for the standard deviation was estimated from the measured values in a period with an essentially constant hydrogen consumption rate. Constant values were taken as it was assumed that the deviations were mainly caused by fluctuations which are independent of the measured uptake rates. The normal distribution assumption was checked by a normal probability plot (data not shown).

As quality indicator for the fit of models, 'reduced  $\chi^2$ ' values were calculated (Table 3).<sup>[13]</sup> Moreover, modeling results were evaluated by judging the obtained residual plots. Residuals in the plots were weighed by the estimated standard deviations of the measurements. Accuracy bounds on the model parameters were calculated from the diagonal of the estimated covariance-matrix for each parameter.<sup>[14]</sup>

## Acknowledgements

We wish to thank Jens Wöltinger and Dietmar Reichert (Degussa AG, Hanau, Germany) for the kind gift of catalyst and discussion; Andreas Franz, Daniela H. Müller, and Christian R. Reimers (all of Forschungszentrum Jülich) for skilful technical support. We both thank Christian Wandrey (Forschungszentrum Jülich) for his continuous support. Our research was facilitated by financial support from the German Federal Ministry of Education and Research (BMBF) and Degussa AG.

## References and Notes

- [1] a) J. M. Brown, in: *Comprehensive Asymmetric Catalysis*, Vol. I, Chapter 5.1, (Eds.: E. N. Jacobsen, A. Pfaltz, H. Yamamoto), Springer, Berlin, **1999**, p. 121; b) W. S. Knowles, *Angew. Chem. Int. Ed.* **2002**, *41*, 1998; c) R. Noyori, *Angew. Chem. Int. Ed.* **2002**, *41*, 2008.
- [2] a) B. Cornils, W. A. Herrmann, *J. Catal.* **2003**, *216*, 23; b) H.-U. Blaser, F. Spindler, M. Studer, *Appl. Catal. A:*

- General* 2001, 221, 119; c) W. Locke, *The Alchemist* 2001, January <http://www.chemweb.com/alchem/articles/985883680391.html>.
- [3] C. de Bellefon, N. Tanchoux, D. Schweich, *Proceedings of The Second European Congress on Chemical Engineering (ECCE 2)*, 1999.
- [4] a) Y. Sun, R. N. Landau, J. Wang, C. LeBlond, D. G. Blackmond, *J. Am. Chem. Soc.* 1996, 118, 1348; b) Y. Sun, J. Wang, C. LeBlond, R. N. Landau, J. Laquidara, D. G. Blackmond, *J. Mol. Cat. A* 1997, 115, 495.
- [5] a) C. R. Landis, J. Halpern, *J. Am. Chem. Soc.* 1987, 109, 1746; b) J. Halpern, *Science* 1982, 217, 401; c) A. S. C. Chan, J. J. Pluth, J. Halpern, *J. Am. Chem. Soc.* 1980, 102, 5952; d) K. Burgess, X. Cui, *J. Am. Chem. Soc.* 2003, 125, 14212; e) J. A. Osborn, F. H. Jardin, J. F. Young, G. Wilkinson, *J. Chem. Soc.* 1966, 1711; f) R. Hartmann, P. Chen, *Adv. Synth. Catal.* 2003, 345, 1353.
- [6] a) A. Börner, D. Heller, *Tetrahedron Lett.* 2001, 42, 223; b) C. J. Cobley, I. C. Lennon, R. McCague, J. A. Ramsden, A. Zanotti-Gerosa, *Tetrahedron Lett.* 2001, 42, 7481.
- [7] R. Brereton, *The Alchemist* 2002, April <http://www.chemweb.com/alchem/articles/1015947525148.html>.
- [8] a) U. Nagel, *Angewandte Chemie* 1984, 96, 425; b) U. Nagel, E. Kinzel, *Chem. Ber.* 1986, 119, 1731; c) U. Nagel, E. Kinzel, J. Andrade, G. Prescher, *Chem. Ber.* 1986, 119, 3326; d) U. Nagel, E. Kinzel, *Chem. Ber.* 1986, 119, 1731.
- [9] a) G. E. P. Box, W. J. Hill, *Technometrics* 1967, 9, 57; b) T. El Solh, K. Jarosh, H. de Lasa, *Ind. Eng. Chem. Res.* 2003, 42, 2507.
- [10] a) L. O. Nindakova, B. A. Shainyan, *Russ. Chem. Bull.* 2001, 50, 1855; b) H. B. Kagan, T.-P. Dang, *J. Am. Chem. Soc.* 1972, 94, 6429.
- [11] Half-life time  $t_{1/2}$  of active catalyst is  $t_{1/2} = k_{\text{deact}}^{-1} \ln 2$  in the case of first-order deactivation.
- [12] A. Buchholz, L. Greiner, C. Hoh, A. Liese *J. Capillary Electrophoresis Microchip Tech.* 2002, 7, 51.
- [13] J. R. Taylor, *An introduction to error analysis: the study of uncertainties in physical measurements*, 2nd edn., University Science Books, Sausalito, California, USA, 1997.
- [14] a) A. R. Gallant, *Nonlinear Statistical Models*, John Wiley & Sons, Inc., New York, 1987; b) A. Buchholz, *PhD thesis*, Technische Universität Dresden, Germany, 2000.